Optics & Laser Technology 43 (2011) 806–813

Contents lists available at ScienceDirect

Optics & Laser Technology

journal homepage: www.elsevier.com/locate/optlastec

Microstructure and corrosion behavior of austenitic stainless steel treated with laser

I.Y. Khalfallah [a], M.N. Rahoma [b], J.H. Abboud [a], K.Y. Benyounis [c,*]

[a] Department of Mechanical Engineering, Faculty of Engineering, Garyounis University, Benghazi P.O. Box 1308, Libya
[b] Department of Chemistry, Science College , Garyounis University, Benghazi P.O. Box 1308, Libya
[c] Department of Industrial Engineering, Faculty of Engineering, University of Garyounis , Benghazi 1308, Libya

ARTICLE INFO

Article history:
Received 6 July 2010
Received in revised form
27 October 2010
Accepted 9 November 2010
Available online 13 December 2010

Keywords:
Laser treatment
Corrosion
Microstructure

ABSTRACT

Surface modification of AISI316 stainless steel by laser melting was investigated experimentally using 2 and 4 kW laser power emitted from a continuous wave CO_2 laser at different specimen scanning speeds ranged from 300 to 1500 mm/min. Also, an investigation is reported of the introduction of carbon into the same material by means of laser surface alloying, which involves pre-coating the specimen surfaces with graphite powder followed by laser melting. The aim of these treatments is to enhance corrosion resistance by the rapid solidification associated with laser melting and also to increase surface hardness without affecting the bulk properties by increasing the carbon concentration near the surface. Different metallurgical techniques such as optical microscopy, scanning electron microscopy (SEM), and X-ray diffraction (XRD) were used to characterize the microstructure of the treated zone. The microstructures of the laser melted zones exhibited a dendritic morphology with a very fine scale with a slight increase in hardness from 200 to 230 Hv. However, the laser alloyed samples with carbon showed microstructure consisting of γ dendrite surrounded by a network of eutectic structures (γ+carbide). A significant increase in hardness from 200 to 500 Hv is obtained. Corrosion resistance was improved after laser melting, especially in the samples processed at high laser power (4 kW). There was shift in I_{corr} and E_{corr} toward more noble values and a lower passive current density than that of the untreated materials. These improvements in corrosion resistance were attributed to the fine and homogeneous dendritic structure, which was found throughout the melted zones. The corrosion resistance of the carburized sample was lower than the laser melted sample.

1. Introduction

When a metallic surface is irradiated with a high power laser pulse, part of the energy is reflected and the other is absorbed. The absorbed energy is "instantaneously" transferred to the lattice and rapidly raises the near-surface temperature and reaches the melting point. As a consequence to this, a liquid–solid interface starts to move downward into the metal. As soon as the laser pulse is finished the resolidification process begins from the liquid/solid interface towards the surface. Due to the high cooling rates (10^6 C/s), solid-state diffusion can be neglected and homogeneous and fine solidification microstructures can be achieved with a wide variety of surface compositions without the limitations of conventional processes, for instance, to extend solid solutions and to obtain metastable structures or even metallic glasses. This technique has been widely used to treat surfaces of different ferrous and non-ferrous materials and considerable improvements in corrosion, erosion, and hardness have been reported due to the unique structure obtained after laser melting [1–7]. By coating the metal surface with some elements, usually in the form of powder, followed by laser melting, these alloying elements diffuse rapidly into the melt pool to a desired depth forming an alloyed layer in a short period of time. This technique is known as laser surface alloying (LSA) and by this technique, a desired alloy chemistry and microstructure can be generated on the sample surface. The concept of carburizing by laser melting was initially realized through the use of graphite coatings during laser surface hardening of steels, which served as an efficient way to increase the coupling of radiation with the steel substrate, which for the case of the CO_2 laser far-infrared radiation (wavelength 10.6 m) is extremely low. It was then observed that a substantial amount of carbon could be introduced to steel surfaces in that manner. Since then, studies have been reported on the laser carburizing of commercial pure iron [8], plain carbon [9], and low alloy steel [10].

Laser applications in the surface treatment of stainless steel have been focused on ferritic (AISI 430), martenistic (AISI 420), and austenitic (AISI 304 and AISI 310) types to improve pitting

* Corresponding author.
E-mail addresses: younis_ibrahem@yahoo.com (I.Y. Khalfallah), jhabboud@yahoo.com (J.H. Abboud), kybenyounis@yahoo.com (K.Y. Benyounis).

0030-3992/$ - see front matter © 2010 Elsevier Ltd. All rights reserved.
doi:10.1016/j.optlastec.2010.11.006

corrosion resistance [11–16]. In general, the corrosion resistance was improved after laser melting and it has been found that the corrosion resistance depends critically on the laser processing parameters, particularly for the cases of ferritic and martenisitic. The effect of laser melting of UNS S42000 steel on cavitation erosion and pitting corrosion has been studied in detail by Man and his co-workers [13–15] and Krishna and Bandyopadhyay [16]. It was found that cavitation erosion improved significantly after laser melting due to the formation of large volume fraction of retained austenite, which has high martenisitic transformability; the amount of retained austenite in laser melted surface is found to strongly depend on the laser power and scan speed. The hardness of the melted zone was 27–55% higher than that of conventionally heat treated samples. Similar results were obtained by Tu and his workers [17]. These results present an exciting possibility of surface treatment of martensitic stainless steels using laser. The performance and feasibility of selective laser melting technique to directly fabricate a 316L stainless steel/HA (hydroxyapatite) composite was investigated by [18] to be used as load-bearing and bioactive implants. It was found that an optimum condition exists to fabricate good quality 316L SS/HA composite specimens using a duplicate scanning strategy during the surface laser melting process. The high strength of the SS/HA composite manufactured made laser melting technique highly potential to be employed in bioactive and load-bearing bone implant applications.

Table 1
Nominal chemical composition of steels used in study (wt%).

Element	Fe	C	Cr	Ni	Mn	Si	Mo	P	S
wt%	Bal.	0.08	16–18	10–14	2.0	1.0	3.0	0.045	0.03

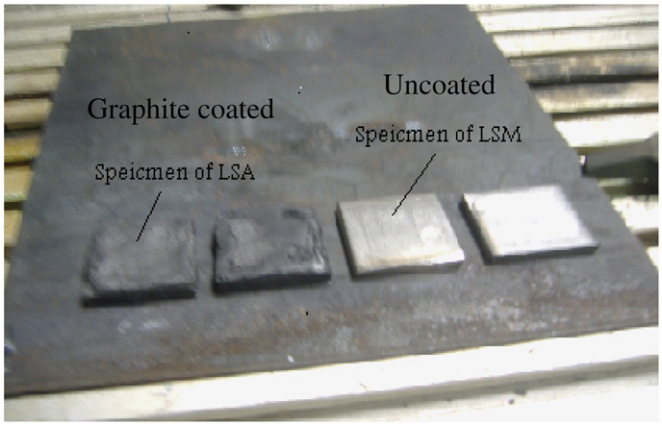

Fig. 1. Photograph shows uncoated and graphite coated specimens before laser melting.

Table 2
Processing parameters used for LSM and LSA.

Specimen no.	Laser power *P* (kW)	Scan speed *V* (mm/min)	Specimen no.	Laser power *P* (kW)	Scan speed *V* (mm/min)
M-13	2	300	A-19	2	300
M-14	2	900	A-20	2	900
M-15	2	1500	A-21	2	1500
M-16	4	300	A-22	4	300
M-17	4	900	A-23	4	900
M-18	4	1500	A-24	4	1500

M—melting; A—alloying with carbon

Fig. 2. Laser system: (a) CO_2 laser, (b) gas control valves, (c) X–Y table, (D) laser focus head, and (E) laser control unit.

The aim of the present work is to study the effect of local surface melting by laser of austenitic 316 steel on corrosion resistance and also to investigate the effect of laser surface alloying of the same material with carbon as a means to increase surface hardness without affecting corrosion resistance.

2. Experimental work

2.1. Material

The austenitic stainless steel used in the present work is AISI 316 supplied by the research center of Tajoura. The material was rolled and annealed to a sheet of 5 mm thickness. The chemical composition is given in Table 1. Several specimens of surface area $15 \times 15\ mm^2$ were prepared using a wire electrical discharge cutting machine. The sample surfaces were polished up to grade 800 to give a consistent surface finish. For laser surface alloying with carbon, a layer of graphite powder having particle size around 5 μm was mixed with a binder and applied as evenly as possible on the polished steel. The deposited graphite thickness was around 100 μm. After graphite coating, the surfaces were ground with 800 grid emery paper to make the surface flat and uniform (Fig. 1).

2.2. Laser

The laser machine used in this investigation is a CO_2 laser operating in a continuous and pulse mode. The maximum output power is 6 kW. The laser beam is focused by Zn Se lens with focal length 200 mm. The minimum diameter of the focused beam is about 0.47 mm. The relative movement between the laser beam and the work piece is realized by CNC (computer numerical control) X–Y–Z nozzle. For alignment procedures, a He Ne laser beam was transmitted along the optical axes (Fig. 2). The distance between the laser beam focus point and the metal surface was kept about 10 mm; this gives a beam diameter of about 2 mm.

2.3. Laser surface melting and alloying

Laser surface melting was carried out using a CW CO_2 laser of maximum power 6 kW. Argon gas flowing at the rate of 900 l/hr was used as the shielding gas to prevent oxidation of the sample. Single and overlapping tarcks were obtained by overlapping of successive melt tracks at 50% track width interval. Laser surface alloying was achieved by surface melting of the 316 steel, which was coated with the graphite powder. Table 2 present the processing parameters used for LSM and LSA. More details on the experimental work can be found in Ref. [19].

2.4. Metallographic examination

After laser treatments, cross sections were obtained by cutting the processed sample perpendicular to the beam direction, in order to allow for the observation below the surface of the materials. A microstructural study was performed by optical microscopy and scanning electron microscopy. The scanning electron microscope (SEM) used was type LEO 1430 VP. The filament type is LaB6, which has higher performance than a tungsten filament. All the micrographs were imaged using secondary electrons. Specimens were etched with a reagent consisting of 25 g $FeCl_3$, 25 ml HCl, and

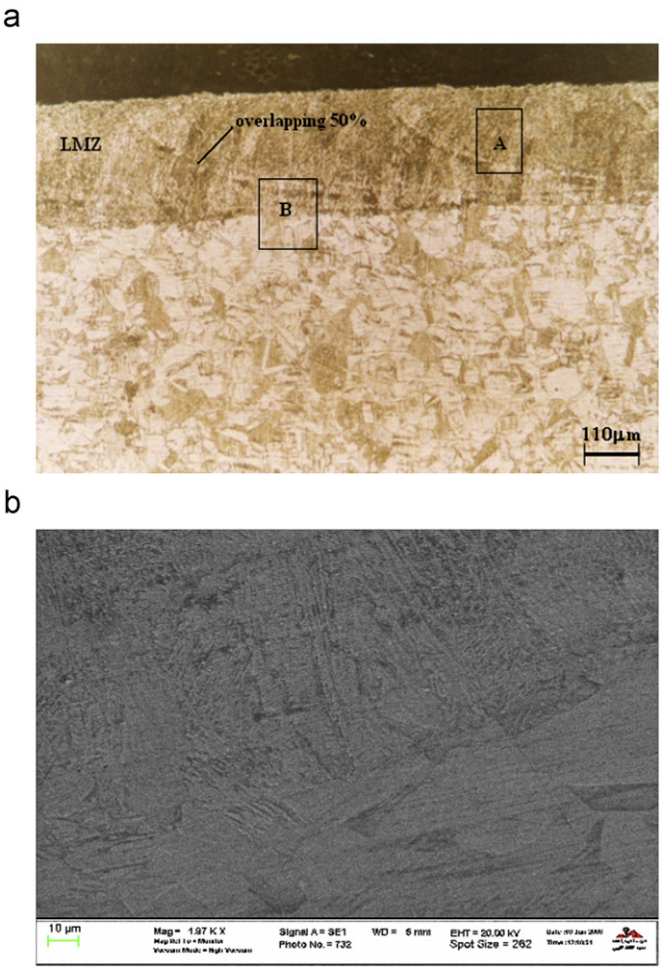

Fig. 4. Optical micrographs show (a) cross section of LMZ and (b) SEM of section B.

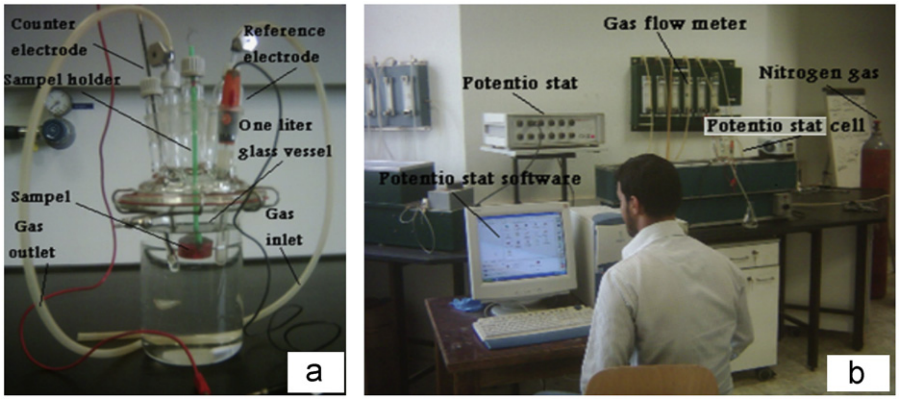

Fig. 3. (a) Corrosion test cell and (b) corrosion test system (potentiostat test).

100 ml H_2O. X-ray diffraction was taken from the surface of the overlapped sample. Microhardness was measured as a function of depth below the surface for the entire laser treated specimen with a microhardness tester. The applied force is 200 gf and 10 s.

2.5. Electrochemical test

Potentiodynamic polarization scans were carried out using a Gill 12 stagnating the pitting corrosion behavior of laser surface modified and as-received specimens. 3.5% NaCl solution was kept at a constant temperature of 23 °C and decreased by purging with nitrogen for 1 h prior to corrosion tests (Fig. 3a–b). A saturated calomel electrode (SCE) was used as the reference electrode and the auxiliary electrode was made of platinum. All data were recorded after an initial delay of 1 h for the specimen to reach a steady state. The reference electrode was commercial saturated calomel electrode (Hg/Hg_2Cl_2 in KCl); the auxiliary electrode was made of platinum. The potentiostat is fully computerized and gives the corrosion rate from I_{corr} multiplied by a metal factor using software attached to the potentiostat.

3. Result and discussion

3.1. Microstructure

Laser surface melting of 316 steel at different laser powers and scanning speeds produce a microstructure consisting of columnar grains grown epitaxially from the interface toward the top surface (Fig. 4a and b). Very fine dendrites were observed within these grains. The secondary arm spacing was estimated to be 2–3 μm suggesting a very high cooling rate achieved during solidification. From the other side, the graphite coated sample showed a melted zone of bigger size compared to the uncoated 316 steel under the same processing conditions (Fig. 5). This is due to the carbon, which leads to improvement in the coupling efficiency between the laser beam and the substrate. It is evident from the micrographs in Fig. 5a and b that graphite powder dissolved completely in the molten pool and no evidence of free graphite was seen, which indicates good mixing and alloying between the graphite powder and the molten substrate. The alloyed zone displays a fine dendritic structure homogeneously distributed in the melted zone (Fig. 5a and b). The region adjacent to the interface showed a planar zone

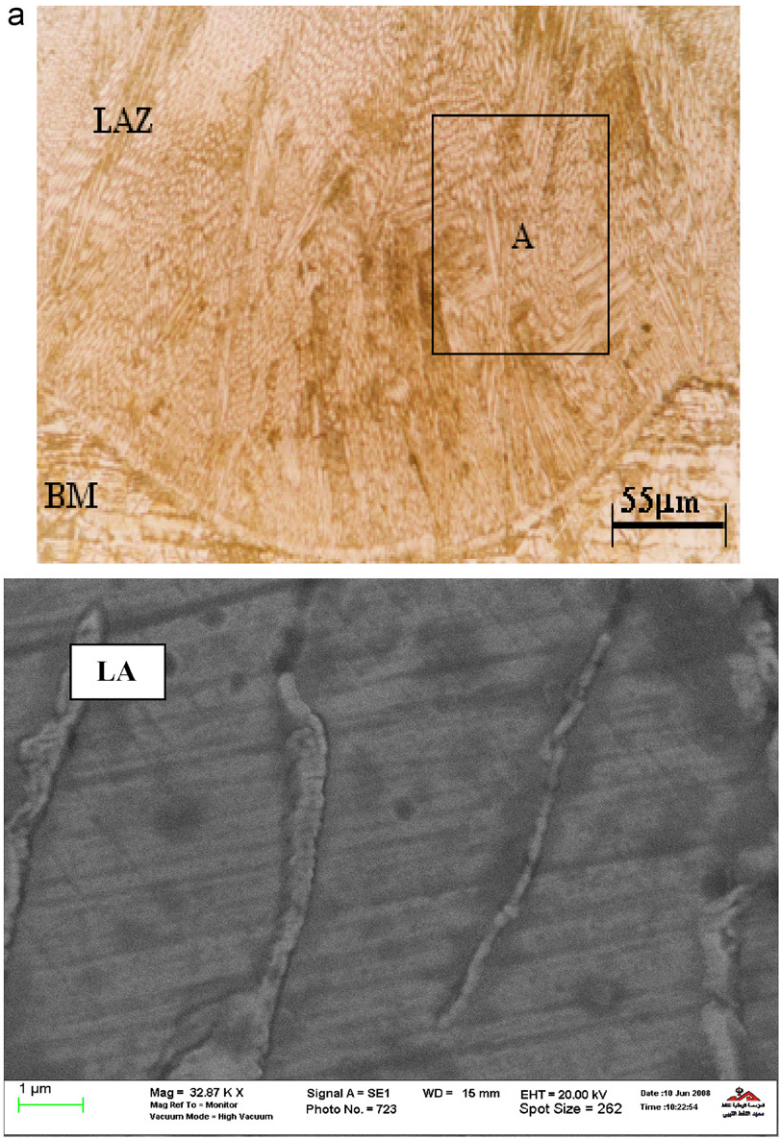

Fig. 5. Optical micrographs show (a) cross section of LAZ and (b) SEM of section A (2 kW and 900 mm/min).

(appeared white), which becomes dendritic as the distance from the interface increases. This change in solidification mode from planar to dendritic can be interpreted on the basis of the temperature gradient and growth rates. The temperature gradient and growth rate are important in the combined forms GR (cooling rate) and G/R since they influence the scale of the solidification substructure and solidification morphology, respectively. Examination of the structure at high magnification revealed a thin layer of a discontinuous carbide network located between the dendrites (Fig. 5b); the average size of the carbides is 0.5 μm. This type of structure resembles a eutectic structure comprising of γ+carbides. Solidification of this alloy commences with the nucleation of austenite in the form of dendrites. During the growth of these dendrites, excess carbon is rejected and accumulated between the dendrites, so the last liquid will solidify as eutectic. The extent of alloying seems to improve when a high power is used. (Fig. 6) shows more interdendritic regions in the sample processed at 4 kW and 1500 mm/min. This means that more carbon dissolves in this sample and consequently more interdendritic eutectic carbide is formed. EDS analysis was performed on this sample using a SEM microscope equipped for EDS analysis. Although carbon analysis is difficult due to the low power energy of the carbon peak, the EDS analysis gave carbon content of about 2 wt% in the sample shown in Fig. 6b and 3 wt% in the sample shown in Fig. 6b. This also led to dilution of chromium and other alloying elements present in this steel.

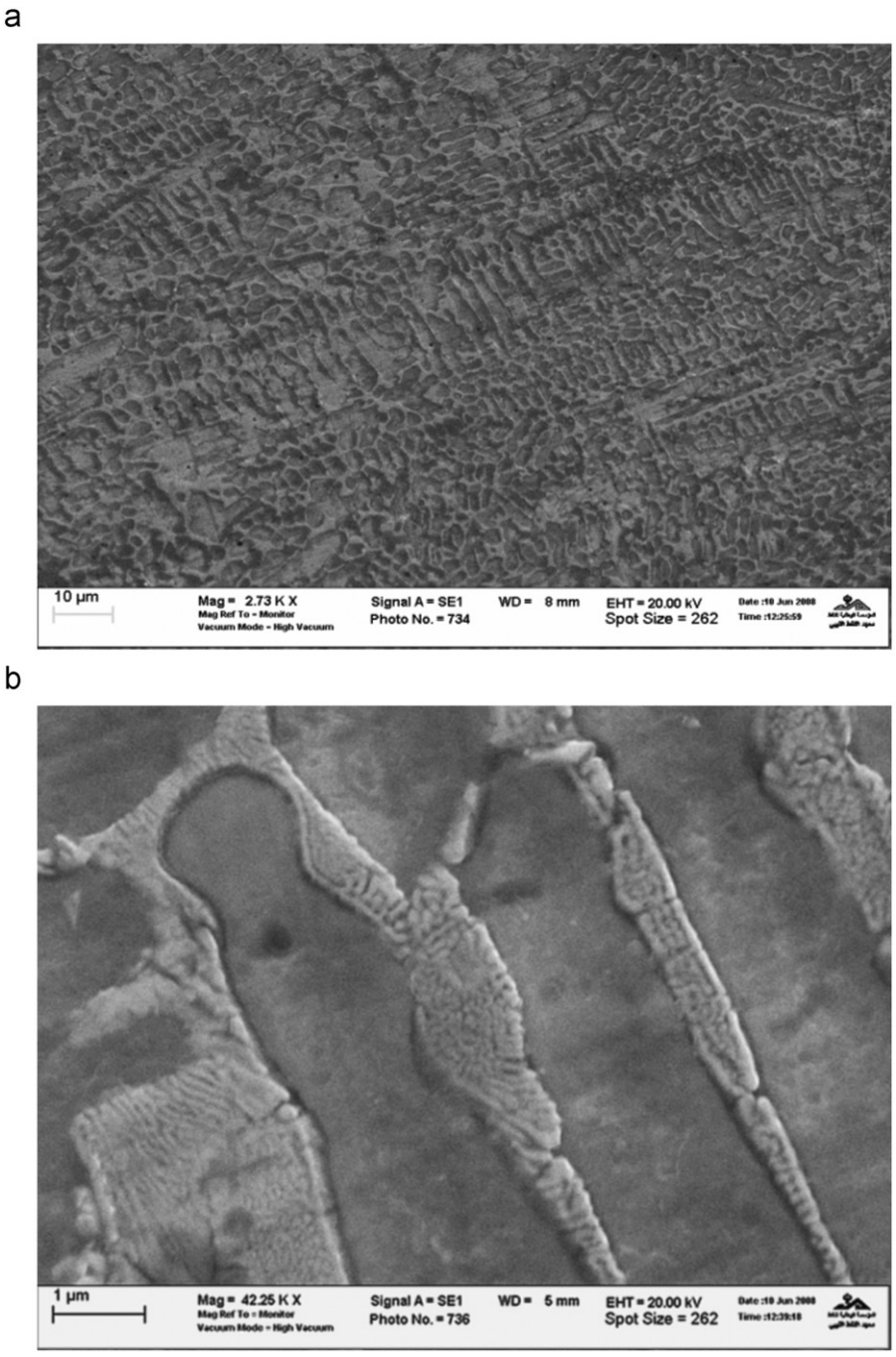

Fig. 6. SEM micrographs show LAZ produced at 4 kW: (a) dendritic structure and (b) interdendritic structure at high magnification.

3.2. X-ray diffraction

X-ray diffraction peaks from the surface of the untreated, surface melted, and surface alloyed samples are shown in Fig. 7a–c. It can be seen that the diffraction peaks from the surface of the laser treated samples were similar to those of untreated 316 steel, suggesting that the major phases have fcc structure. However, there is a shift in the position of peaks of the laser treated samples. This shift is not uniform. The degree of lattice expansion was different for each plane and was the largest for (2 0 0), suggesting no uniformity in the expansion of the cubic lattice. In the laser alloyed sample, apart from the fcc phase, there are other peaks identified as Cr_7C_3. The increase in shift of the expanded austenite peaks in the LSA sample was presumably due to an increase in carbon content in the austenite phase. The diffraction lines of the laser treated samples were slightly broadened compared with that of untreated 316 steel. The observed line broadening is attributed to the presence of the strain and many defects such as dislocations in the surface layer due to high cooling rates and non-equilibrium solidification.

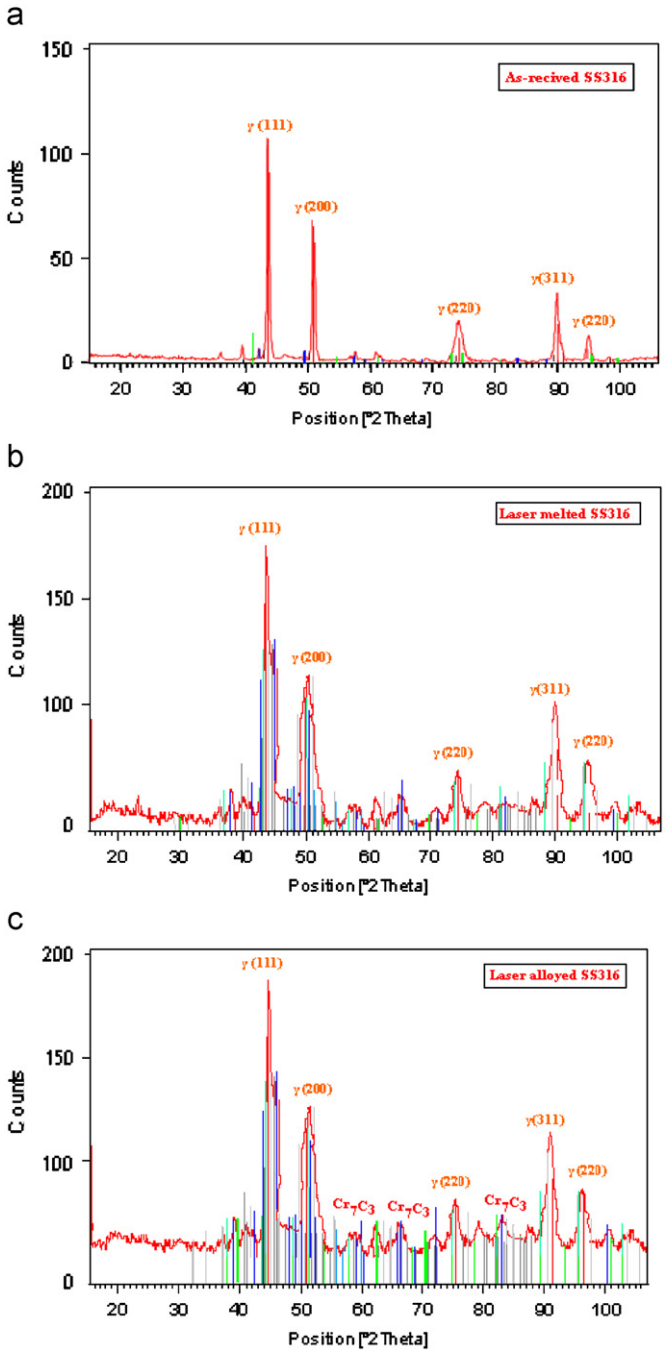

Fig. 7. X-ray diffraction patterns taken from surface of (a) as-received, (b) LMZ, and (c) LAZ (2 kW and 1500 mm/min).

3.3. Microhardness

Microhardness profile across the melted and the alloyed zone is shown in Fig. 8. It is interesting to see that the alloying of carbon leads to a significant increase in hardness especially at high power and also increases the depth to which the hardness extends. At 2 kW, the maximum microhardness was ~470 extended to a distance ~200 μm below the surface followed by a sharp drop in hardness to a value of 200 Hv. At 4 kW, the maximum microhardness was ~500 Hv extended uniformly to a depth of ~500 μm. These results can be interpreted by referring to Fig. 6, which showed a high percentage of interdendritic regions resembling a eutectic structure product consisting of austenite and carbides. The X-ray detects some extra peaks corresponding to Cr_7C_3, which contribute to the hardening effect.

3.4. Corrosion behavior

Table 3 shows the corrosion current I_{corr} and the corrosion rate C.R. of the LSM and LAS samples processed at 2 and 4 kW laser power and 900 mm/min. It is apparent from the table that the C.R. for the LSM sample is lower than that of the as-received material at the two powers level used with more decrease in C.R. at 4 kW. However the situation is reversed when carbon is added to the laser melted zone by the LSA technique. C.R. of the samples alloyed with carbon increases although this increase is small for the sample treated at 4 kW. It can also be seen from Table 3 that the corrosion current increases and becomes higher after (LSA), which may indicate that the addition of carbon to the 316 steel decreases the corrosion protection. The formation of carbide removes chromium from the surface and iron reducing its corrosion resistance. The improvement in corrosion resistance at laser power 4 kW indicates that the processing parameters have a detrimental effect on the improvement of corrosion resistance.

Figs. 9 and 10 show polarization curves for 316 steel in 3.5% w/v sodium chloride solution at ambient temperature after 1 h for LSM

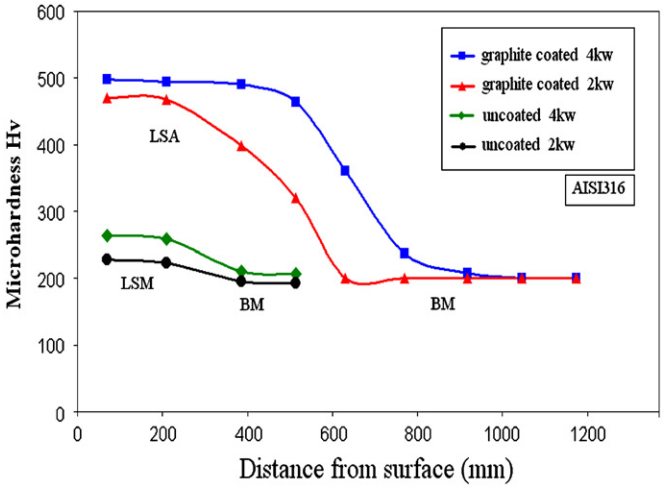

Fig. 8. Microhardness profile across melted and alloyed zone depths produced at scanning speed 900 mm/min and different powers.

Table 3
Corrosion parameter values for AISI 316 steel in 3.5% w/v sodium chloride solution at ambient temperature after one hour.

Specimen no.	Surface condition	Power (kW)	E_{corr} (mV)	I_{corr} (mA/cm^2)	C.R. (mm/year)
M-14	LSM	2	617.343	0.138	0.173
A*-20	LSA	2	362.025	0.167	0.209
M-17	LSM	4	815.411	0.133	0.166
A-23	LSA	4	424.386	0.158	0.198
–	AISI 316	–	563.038	0.142	0.178

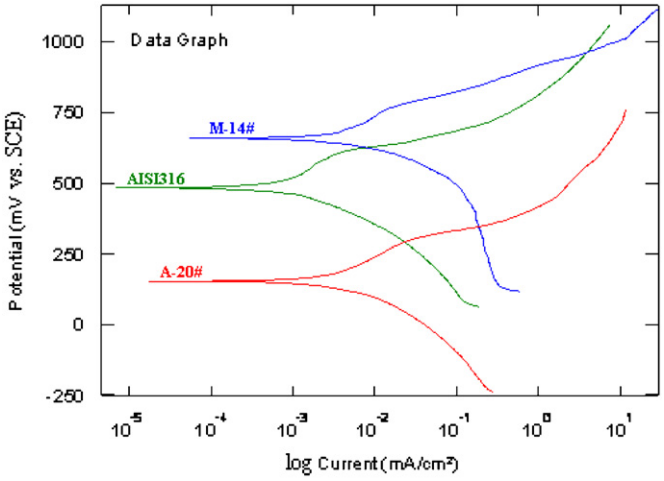

Fig. 9. Polarization curves for 316 steel in 3.5% w/v sodium chloride solution at ambient temperature after 1 h under laser conditions 2 kW and 900 mm/min.

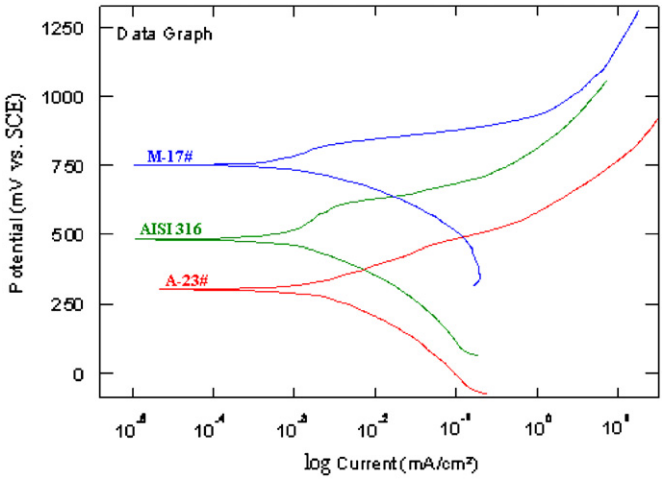

Fig. 10. Polarization curves for 316 steel in 3.5% w/v sodium chloride solution at ambient temperature after one hour under laser conditions 4 kW and 900 mm/min.

and LSA processed at 2 and 4 kW, respectively. It is clear that there was a shift in corrosion potential E_{corr} to more positive values in the case of LSM. This effect is due to the inhibiting effect of the self protective layer formed on the surface of the steel samples. It can be seen that the addition of carbon (LSA) shifts E_{corr} to more negative potentials and also increases the corrosion current value I_{corr}.

It can be seen from Fig. 10 that 316 steel has the same behavior as in Fig. 9, which is due to the fact that it has the same corrosion mechanism in both laser conditions laser power 2 kw and scanning speed 900 mm/min. (Table 3). It can be seen that the addition of carbon (LSA) shifts E_{corr} to more negative potentials and also increases the corrosion current value (I_{corr}), which confirms the suggestion of the formation of carbide removing chromium from the surface and iron reducing its ability to form a protective layer, which reduces the corrosion. However this decrease in corrosion behavior is not severe taking into account the significant increase in surface hardness from 200 to 500 Hv.

4. Conclusions

In the present investigation, the laser surface melting technique by laser irradiation is investigated as a process capable of producing surfaces with a unique microstructure and homogeneity and as a consequence surface properties such as hardness and corrosion might improve. The following conclusions were obtained:

- Laser surface melting of 316 austenitic stainless steels using 2 and 4 kW allows obtaining a homogeneous modified surface layer with a very fine dendritic structure. The microhardness was not increased after melting treatment but corrosion resistance improved especially when a high power is used. There was a shift in I_{corr} toward a lower and more noble values after this treatment.
- Laser surface alloying by incorporating carbon into the laser melted zone produced a modified layer consisting of austenite dendrites surrounded by eutectic carbides. The solidified microstructure is dependent on the mixed carbon content. The microhardness increases significantly after laser alloying from 200 to 500 Hv. High hardness is associated with high carbon content.
- X-ray diffraction analysis confirms that there was no change in the crystal structure after laser melting. There was a shift in the position of the peaks. However, after laser alloying another peak identified as Cr_7C_3 is detected coexisting with the austenite phase.
- The technique of laser alloying with carbon leads to the production of a hard surface but with a corrosion resistance inferior to that of the base metal.
- Surface melting improves the corrosion resistance where the surface alloying increases the corrosion rate. Better corrosion resistance is obtained when this steel is treated at high power.

Acknowledgments

Acknowledgments are made to Husham Al-Mukherim in the laser research center in Tripoli for carrying out the laser treatment and to the corrosion laboratory in the Gulf company, especially Eng. Aead Algderi and Mr. Daoud Alabare for allowing us to conduct the corrosion test.

References

[1] Ayers JD, Schaefer RJ, Tucker TR. In: White CA, Peercy PS, editors. Laser and electron beam processing of materials. New York: Academic Press; 1980. p. 749.
[2] Steen WM. Laser surface treatment of metals. In: Draper CW, Mozzoldi P, editors. NATO ASI series, vol. 100. Kluwer Academic; 1986.
[3] Steen WM. Laser cladding, alloying, and melting. In: Belforte D, Leritt M, editors. Tulsa, OK: Penwell Publishing Company; 1983.
[4] Ayers JD. Laser in metallurgy. In: Mukherjee Mazumdar J, editor. Warrendale, PA: The Metallurgical Society of AIME; 1981. p. 279.
[5] Mordike BL. Surface modification of metals. In: Cahn RW, editor. Materials science and technology, vol. 15. Processing of metals and alloys. Berlin: VCH; 1991. p. 36.

[6] Sun Z, Annergren I, Pan D, Mai TA. Effect of laser surface remelting on the corrosion behavior of commercial pure titanium sheet. Materials Science and Engineering A 2003;345:293–300.
[7] Fakron OMA, Abboud JH. Surface melting of nodular cast iron by Nd–YAG laser and TIG. Journal of Materials Processing Technology 2005;170:127–32.
[8] Walker A, West DRF, Steen WM. Laser surface alloying of iron and 1C–1.4Cr steel with carbon. Metal Technology 1984;11:399–404.
[9] Abboud JH, Benyounis KY, Olabi AG, Hashmi MSJ. Laser surface treatments of iron-based substrates for automotive application. Journal of Materials Processing Technology 2007;182:427–31.
[10] Katsamas AI, Haidemenopoulos GN. Laser-beam carburizing of low alloy steel. Surface and Coating Technology 2001;139:183–91.
[11] Conde A, Colaco R, Vilar R, Damborenea J. Corrosion behaviour of steels after laser surface melting. Materials and Design 2000;21:441–5.
[12] Damborenea.J, Marsden.CF, West.DRF, Vazquez.AJ. Pitting resistance of 420 stainless steel after laser melting treatment. In: Proceedings of the ninth European congress on corrosion, vol. 1. Paper FU-172. Utrecht, Holand; 1989.
[13] Kwok CT, Man HC, Cheng FT. Cavitation erosion and pitting corrosion behviour of laser surface melted martensitic stainless steel UNS S42000. Surface and Coatings Technology 2000;126:238–55.
[14] Kwoka CT, Lo KH, Cheng FT, Man HC. Effect of processing conditions on the corrosion performance of laser surface-melted AISI 440C martensitic stainless steel. Surface and Coatings Technology 2003;166:221–30.
[15] Lo KH, Cheng FT, Man HC. Laser transformation hardening of AISI 440C martensitic stainless steel for higher cavitation erosion resistance. Surface and Coatings Technology 2003;173:96–104.
[16] Krishna BVamsi, Bandyopadhyay Amit. Surface modification of AISI 410 stainless steel using laser engineered net shaping. Materials and Design 2009;30:1490–6.
[17] Xuan Fu-Zhen, Huang Xiaoqing, Tu Shan-Tung. Comparisons of $30Cr_2Ni_4MoV$ rotor steel with different treatments on corrosion resistance in high temperature water. Materials and Design 2008;29:1533–9.
[18] Hao L, Dadbakhsh S, Seaman, Felstead M. Selective laser melting of a stainless steel and hydroxyapatite composite for load-bearing implant development. Journal of Materials Processing Technology 2009;209:5793–801.
[19] Algathafi Ibrahem Y. Influence of laser surface melting of austenitic stainless steel on the microstructure and corrosion properties. MSc thesis. Department of Mechanical Engineering, University of Garyounis, Libya, 2008.